

ELLIPTICAL GALAXIES FROM
COSMOLOGICAL
HYDRODYNAMICAL SIMULATIONS

R. Domínguez-Tenreiro

J. Oñorbe

H. Artal

Universidad Autónoma de Madrid, Spain

A. Serna

Universidad Miguel Hernández, Elche, Spain

June 2006

INTRODUCTION

Next challenge: understanding galaxy formation in a cosmological context.

ORIGIN OF EARLY-TYPE GALAXIES

WHY ELLIPTICALS?

Elliptical galaxies are the easiest to study

- Form the most homogeneous family and show the most precise regularities: correlations (power-law).
- SDSS elliptical sample confirms previous correlations: involving
 1. structural and kinematical parameters: the Fundamental Plane relation (FP, Bernardi et al. 2003) and its projections
 2. colors and chemical abundances, for example the $[\alpha/\text{Fe}]$ trend with $\sigma_{\text{los},0}$ (Jorgensen 1999).

MORE SPECIFICALLY

- When were their stellar populations born? Where?
- When was their mass assembled?

VERY CONVENIENT: study this problem in connection with the global cosmological model

Self-consistent Approach

Through N-body + Hydro Simulations

TWO SCENARIOS

- demand short formation time-scales and old formation ages for the bulk of the stellar populations of ellipticals
⇒ MONOLITHICAL COLLAPSE SCENARIO
- But range in ages
dynamical peculiarities
⇒ RECENT MERGER EVENTS!!
(discussions in Peebles 2002; Matteucci 2003; Somerville et al. 2004)

THE CODE

DEVA code (Serna, Domínguez-Tenreiro & Sáiz, 2003)

- GRAVITY: AP3M-like
- HYDRODYNAMICS: SPH with (**S-DEVA**) and without (**nonS-DEVA**) ∇h terms considered (energy, entropy and angular momentum conservation)
- TIME STEPPING: Individual timesteps for dynamical or hydro integration (to save CPU time, allowing a good time resolution)
- COOLING: Updated at each step for all particles
- Individual mass particles

THE SIMULATIONS

- 64^3 DM particles and 64^3 GAS particles in a periodic box of 10 Mpc side; $\epsilon_g = 2,33$ kpc
 $\simeq 35.000$ integration timesteps for denser objects
1 baryon (DM) particle: $2.67 \times 10^7 M_\odot$ ($1.29 \times 10^8 M_\odot$).
- No MASS RESAMPLING
- Cosmological models: Λ CDM, \sim **CONSISTENT WITH OBSERVATIONS**
 $\sigma_8 = 1,18$ higher than WMAP or SDSS data, to allow for EARLY-TYPE-LIKE OBJECTS formation (Evrard, Silk and Szalay, 1990).
- Star Formation **Phenomenological parametrization**. Threshold gas density, $\rho_{g,\text{thres}}$ and an efficiency parameter, c_* , determining the SF timescales according with a Kennicutt-Schmidt-law-like algorithm, $t_{\text{SF}} = c_* t_{\text{dyn}}$ (Kennicutt 1998)

Five Simulations: $c_* = 0.3$, $\rho_{\text{thres}} = 6,0 \times 10^{-25}$ **SF-A ELO sample**

Five Simulations: $c_* = 0.1$, $\rho_{\text{thres}} = 1,8 \times 10^{-24}$ **SF-B ELO sample**

ELOs & COSMOLOGICAL SIMULATIONS

ELO Samples:

♠ Pick up dynamically relaxed non-rotating objects, with prominent stellar spheroidal component, no discs, very few gas **ELO = elliptical-like-objects**
SF-A (SF-B) sample: 26 (17) ELOs

♠ Measure **ELO parameters**

3D quantities:

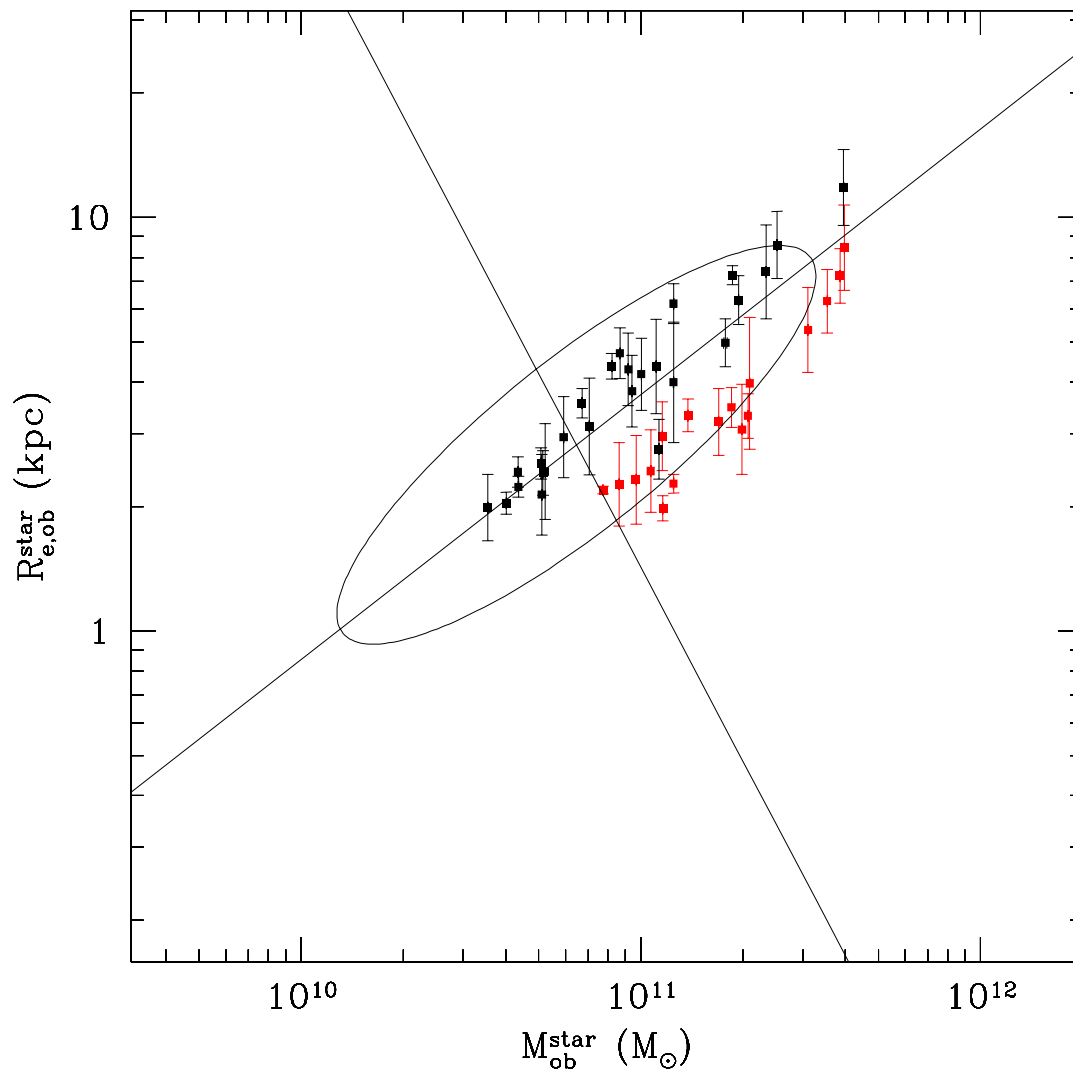
$$M_{\text{bo}}^{\text{star}}, r_{\text{e,bo}}^{\text{star}}, \sigma_{3,\text{bo}}^{\text{star}}$$

projected quantities: stellar half-mass radii, $R_{\text{e,bo}}^{\text{star}}$,
 $\sigma_{\text{los},0}^{\text{star}}$

COMPARING WITH SDSS DATA

- Bernardi et al. (2003b): maximum-likelihood estimates of the parameters characterizing the joint probability distribution for absolute luminosities, M , (the logarithms of) projected sizes, R , and central velocity dispersions, V
- Kauffmann et al. (2003) stellar-mass-to-light ratio constant for early-type galaxies $S \simeq 0,53$ and $S \simeq 0,25$, with dispersions $\sigma_S < 0,15$ and 0.1, (r and z SDSS bands)

- SDSS data can be put in stellar masses instead of absolute luminosity, effective radii and velocity dispersion variables

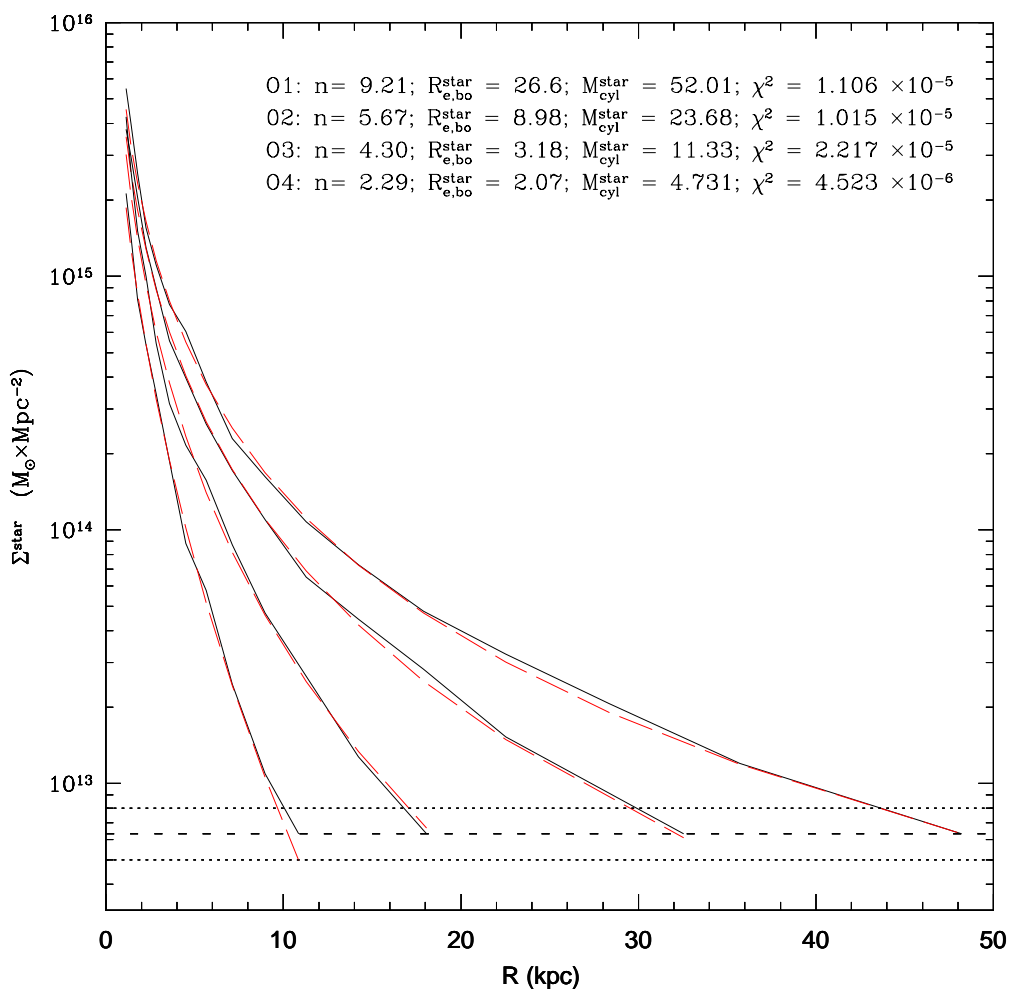


(from [Oñorbe et al. 2006](#)). Projected stellar half-mass radii $R_{e,bo}^{star}$ versus stellar masses M_{bo}^{star} for ELOs. We also draw the concentration ellipse for Bernardi et al.'s (2003b) sample in the z band.

- ♠ Measure ELO projected stellar mass profiles
 - ⇒ surface brightness profile, if the stellar mass-to-light ratio γ^{star} is constant.

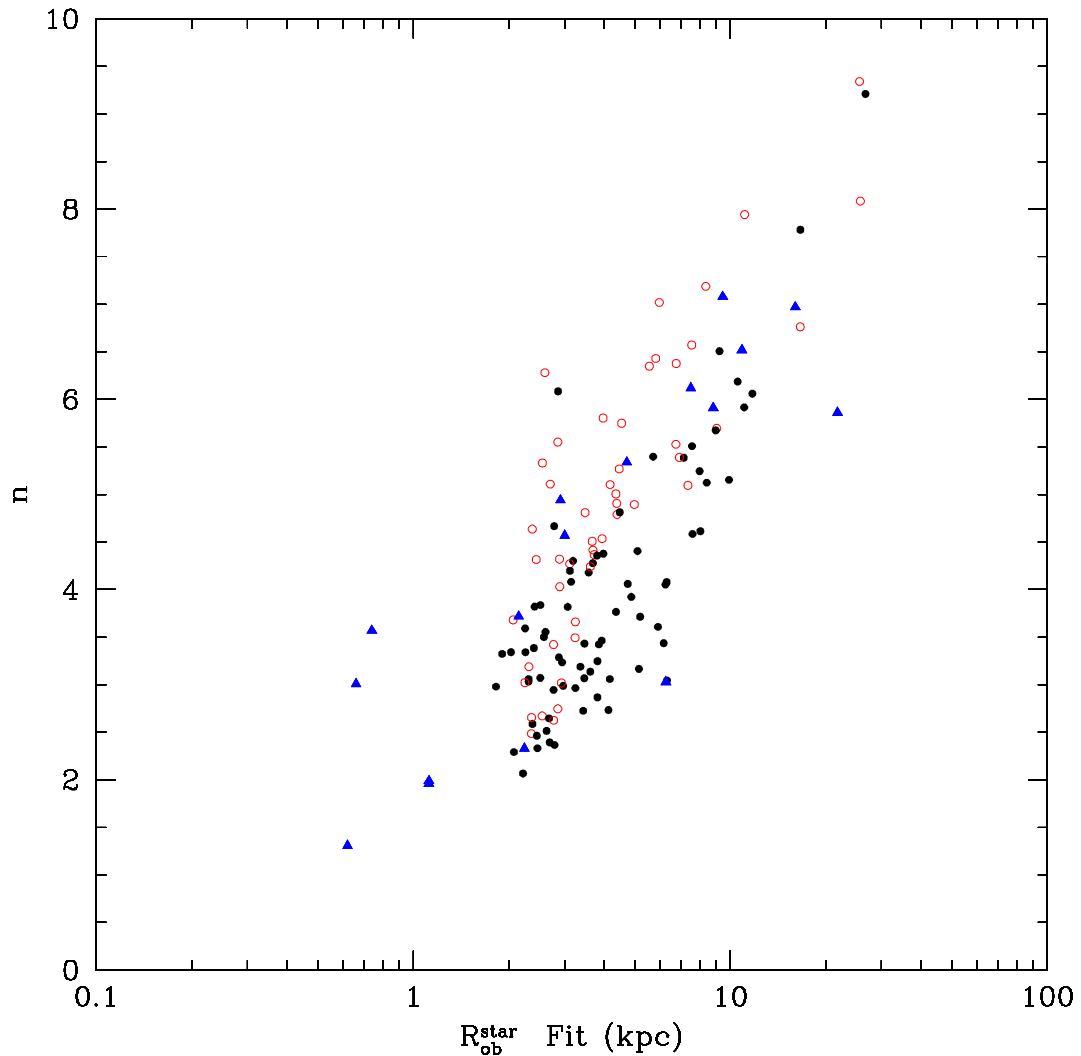
Sèrsic law (Sèrsic 1968), shape parameter n :

$$I^{\text{light}}(R) = I_0^{\text{light}} \exp[-b^n (R/R_e^{\text{light}})^{1/n}] = \Sigma^{\text{star}}(R) / \gamma^{\text{star}}$$



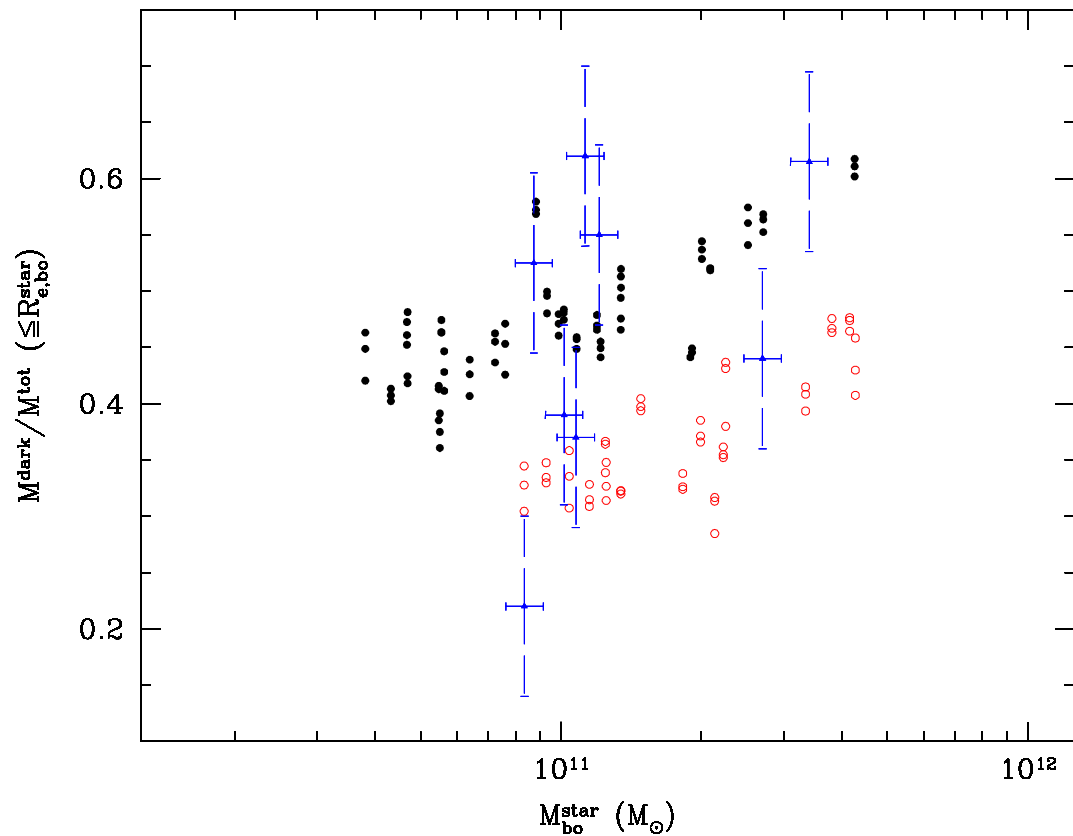
Projected stellar mass density profiles $\Sigma^{\text{star}}(R)$ for different ELOs along with their best fit by a Sèrsic law. The corresponding shape parameter best values and minimal χ^2 per-degree-of freedom are also shown ($\gamma^{\text{star}} = 6,3$)

■ n versus size



The Sersic shape parameter n versus the projected stellar half-mass radii R_{bo}^{star} for SF-A sample (filled symbols) and SF-B sample (open symbols) ELOs. Filled triangles are data on n and R_e^{light} from D'Onofrio (2001)

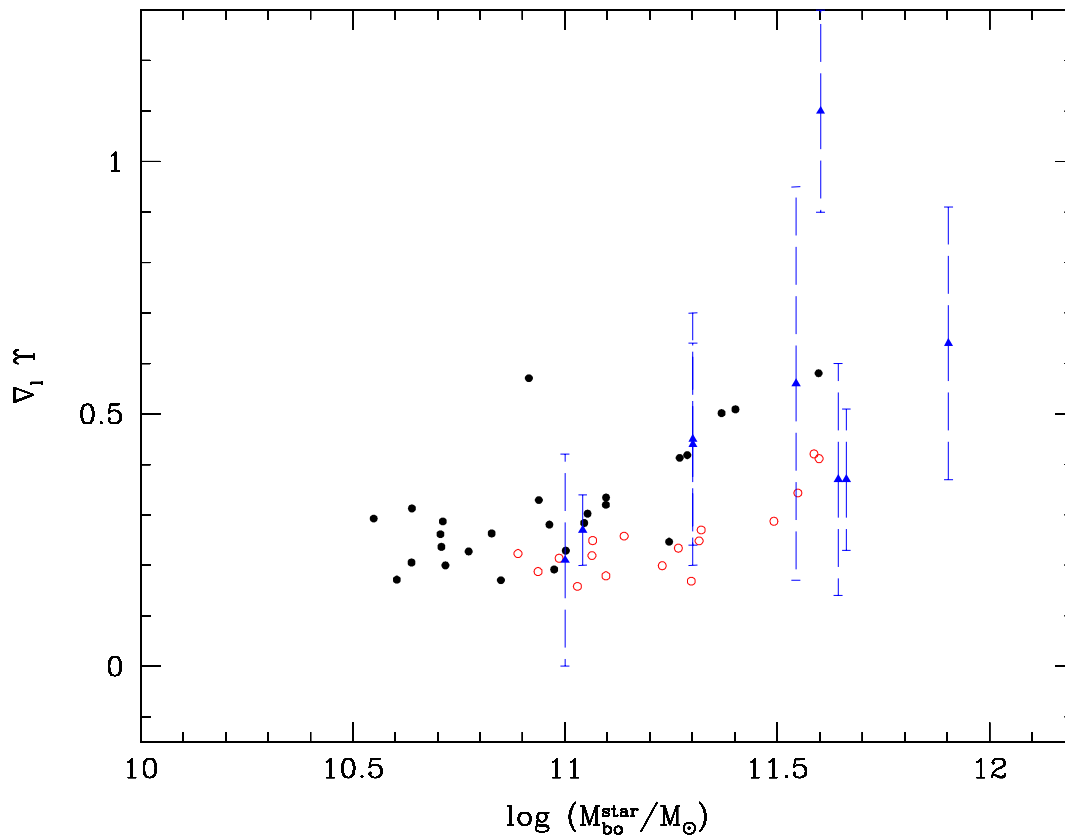
- ♠ Measure the dark matter fraction at the central regions of ellipticals.



The fraction of dark-to-total mass $M^{\text{dark}}/M^{\text{tot}}$ at $r/R_{e,\text{bo}}^{\text{star}} = 1$ versus the ELO stellar masses. Points are the values corresponding to the SAURON sample of ellipticals (Capellari et al. 2005)

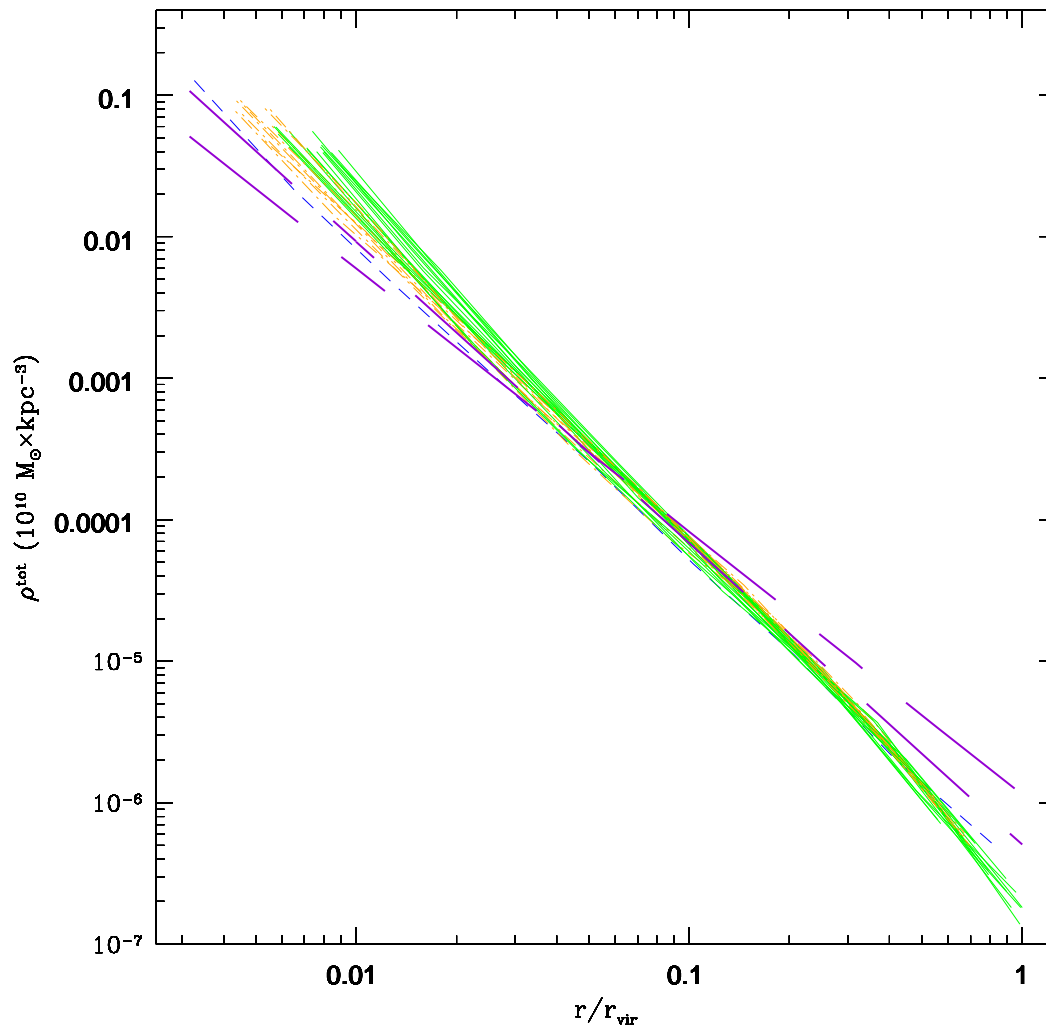
Homology breaking in the dark- versus bright-mass distribution

♠ Measure the gradients of the $M^{\text{dark}}(< r)/M^{\text{star}}(< r)$ profiles.



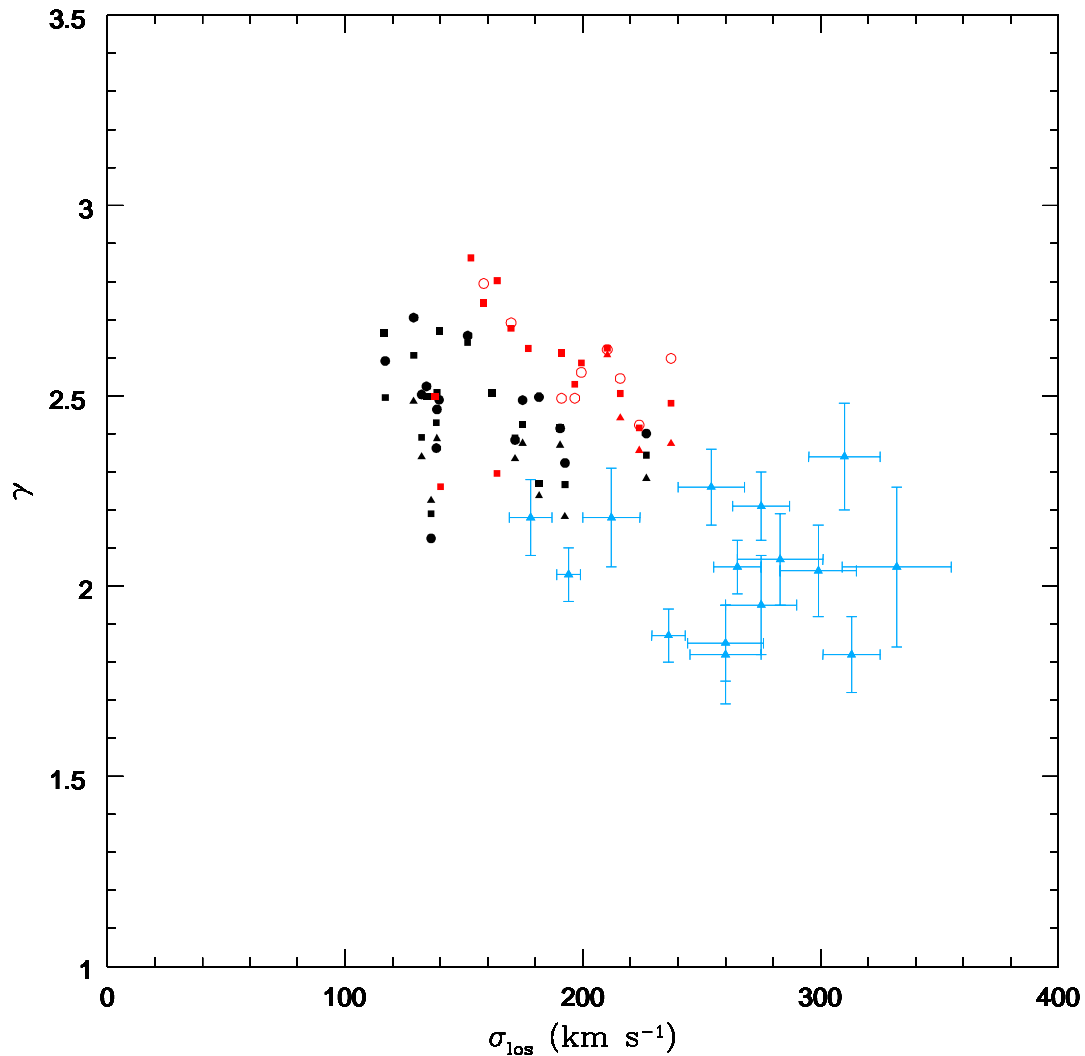
The gradients of the $M^{\text{dark}}(< r)/M^{\text{star}}(< r)$ profiles as a function of their stellar masses (units are solar masses); blue symbols with error bars are the empirical mass-to-light gradients as determined by Napolitano et al. 2005 for galaxies with the a_4 shape parameter lower than 0.1 (that is, excluding fast rotators)

- ♠ Analyze the total mass density profiles
Power law over a large range in r/r_{vir}



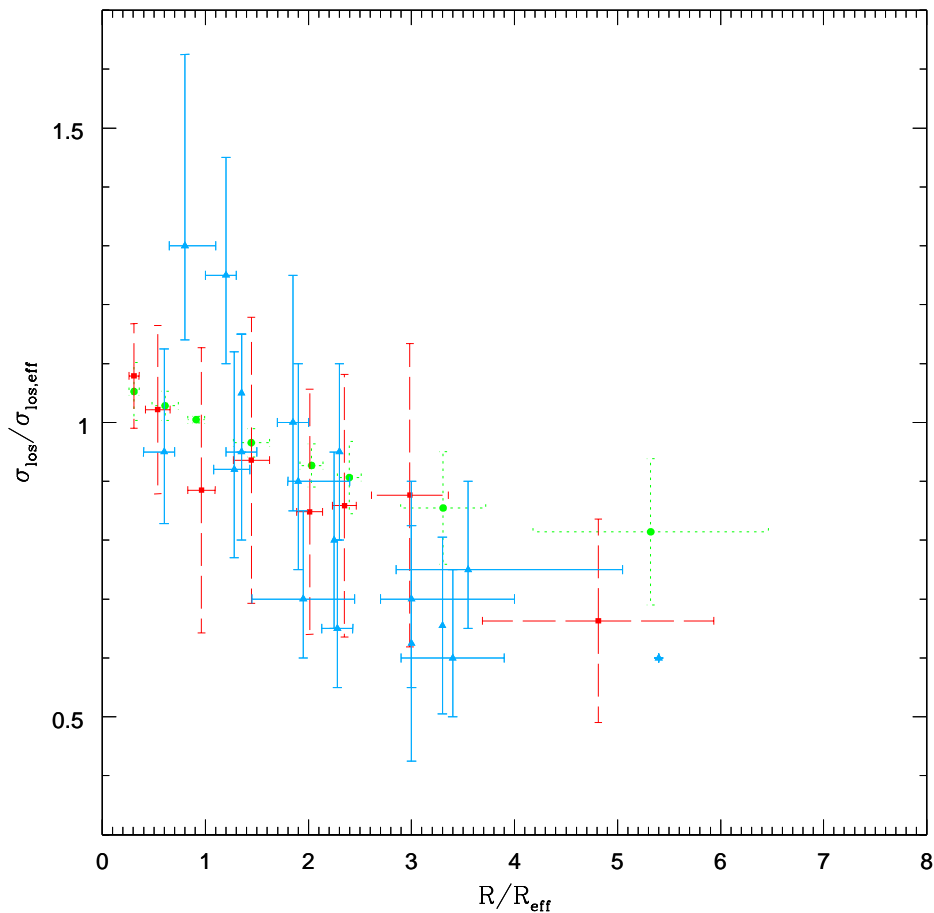
The total mass density profiles for ELOs in the SF-A sample. Green full lines: ELOs with $M_{\text{vir}} < 1,5 \times 10^{12} M_{\odot}$; orange point-dashed lines: ELOs with $1,5 \times 10^{12} M_{\odot} \leq M_{\text{vir}} < 5 \times 10^{12} M_{\odot}$; blue dashed lines: ELOs with $5 \times 10^{12} M_{\odot} \leq M_{\text{vir}}$.

♠ Measure the 3D total mass density profiles
 $\rho^{\text{tot}}(r) \propto r^{-\gamma}$.



The logarithmic slopes corresponding to the total mass density profiles for ELOs in the SF-A (black symbols) and the SF-B samples (red symbols) versus their central L.O.S. stellar velocity dispersions. The fitting range is $r < R_{\text{e,bo}}^{\text{star}}$. Triangles with error bars correspond to data on SLACS lens ellipticals, as given in Koopmans et al. (2006)

♠ Analyze the LOS velocity dispersion profiles at large radii. Declining!!



The SFA sample average LOS velocity dispersion profiles normalized to their values at $R_{e,\text{bo}}^{\text{star}}$ for each ELO (green points) along with their 1σ dispersions. Orange points and error bars: the same for the young stellar particles, with the same normalization. Blue triangles and error bars: data on PN velocity dispersions for NGC 821, NGC 3379, NGC 4494 and NGC 4697 disk galaxies, normalized as in Dekel et al. 2005.

ELOs have counterparts in the real world (structure and dynamics)

THE FUNDAMENTAL PLANE AT $z=0$

- OBSERVATIONS

Effective radius, R_e^{light} , mean surface brightness within that radius, $\langle I^{\text{light}} \rangle_e$, central line-of-sight (los) velocity dispersion $\sigma_{\text{los},0}$ define a plane

$$\log_{10} R_e^{\text{light}} = a \log_{10} \sigma_{\text{los},0} + b \log_{10} \langle I^{\text{light}} \rangle_e + c. \quad (1)$$

with $a \simeq 1,5$, $b \simeq -0,77$ for the SDSS (Bernardi et al. 2003)

Observed FP tilted relative to the virial one

WHY??

WHAT ABOUT ELOs?

♠ $\Sigma^{\text{star}}(R) = \gamma^{\text{star}} I^{\text{light}}(R)$, can be taken as a measure of the surface *brightness* profile



$R_{e,\text{bo}}^{\text{star}}, \langle \Sigma^{\text{star}} \rangle_e, \sigma_{\text{los},0}^{\text{star}}$
DEFINE A DYNAMICAL FP

Free of stellar effects...

Transform to a κ -like orthogonal coordinate system, the dynamical κ_i^{D} system, $i=1,2,3$, (Bender, Burstein & Faber 1992)

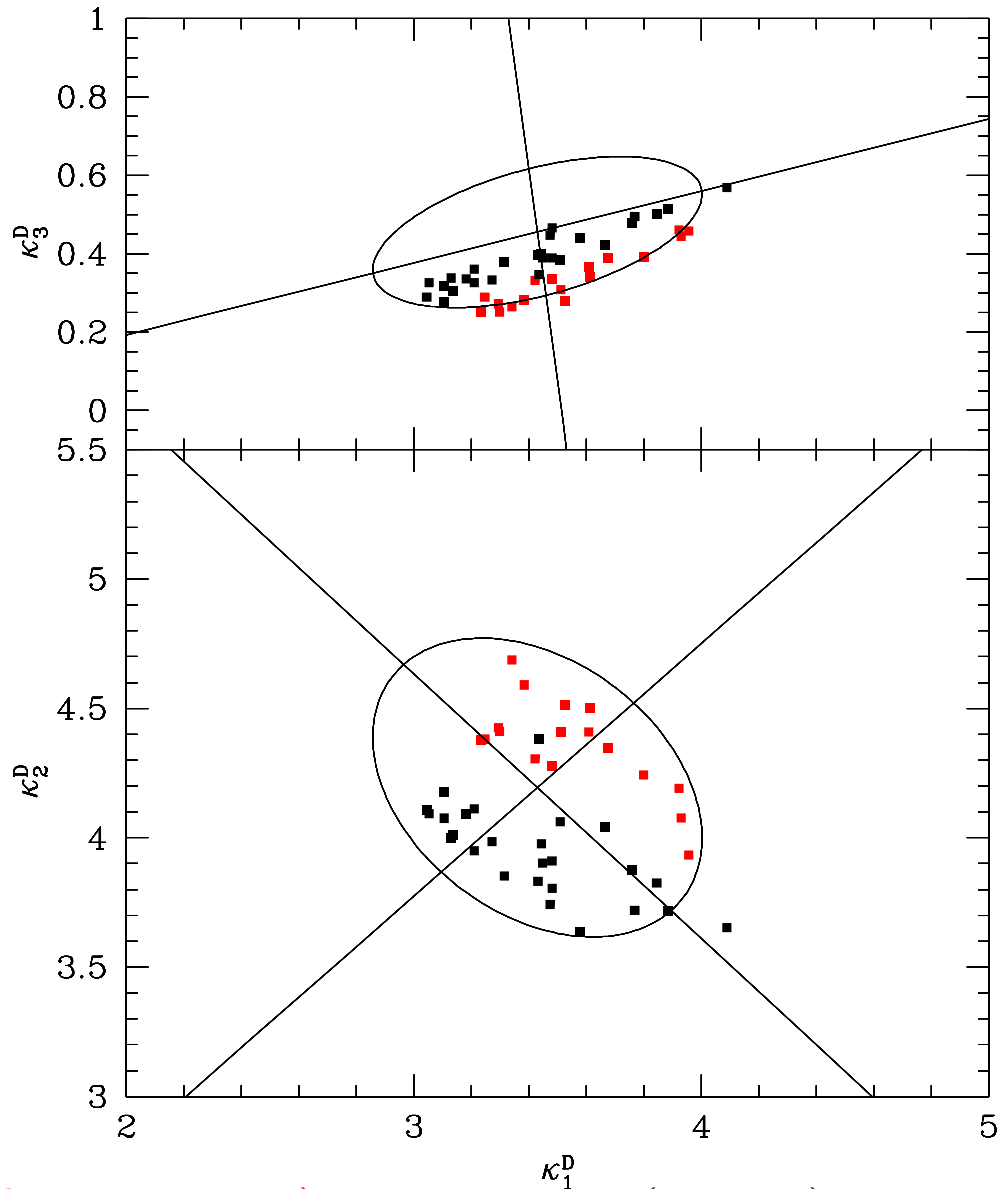
$$\begin{aligned}\kappa_1 &\simeq \kappa_1^{\text{D}}, \\ \kappa_2 &\simeq \kappa_2^{\text{D}} - \sqrt{6}/3 \log M_{\text{bo}}^{\text{star}}/L, \\ \kappa_3 &\simeq \kappa_3^{\text{D}} + \sqrt{3}/3 \log M_{\text{bo}}^{\text{star}}/L\end{aligned}$$

We get

- Good scaling behaviour
- Slope independent of SF parameters
- Zero-point depends on SF parameters through ELO sizes

Moreover,

ELO dynamical FP OK with SDSS sample



(from Oñorbe et al. 2005) Edge-on projection (top panel) and nearly-face-on projection (bottom panel) of the dynamical FP of ELOs in the κ^D variables (black: SF-A sample; red: SF-B sample). We also draw the respective concentration ellipses (with their major and minor axes) for the SDSS early-type galaxy sample from Bernardi et al. (2003b) in the z -band

THE PHYSICS OF THE TILT

ANSWERS (Oñorbe et al. 2005; see poster).
Systematic trends with mass scale in:

♠ **DM vs bright matter content**

$M_{\text{vir}}/M_{\text{bo}}^{\text{star}} \propto (M_{\text{bo}}^{\text{star}})^{\beta_{\text{vir}}}$ with $\beta > 0$: the mass fraction of stars decreases with the mass scale (as suggested by Renzini & Ciotti 1993)

♠ **DM vs bright matter distribution**: homology breaking in the dark- versus bright-mass distribution, mainly because $c_{\text{rD}} \equiv r_{\text{e,h}}^{\text{tot}}/r_{\text{e,bo}}^{\text{star}}$ decreases with the mass scale (as suggested by Guzmán et al. 1993)

Both due to a systematic decrease, with increasing ELO mass, of the relative amount of dissipation experienced by the baryonic mass component along ELO formation

THE SCATTER OF THE FP

Determine the orthogonal scatter through the 3×3 covariance matrix in the 3D variables $E \equiv \log M_{\text{bo}}^{\text{star}}$ (or $\log L$), $R \equiv \log R_{\text{e,bo}}^{\text{star}}$ $V \equiv \log \sigma_{\text{los},0}^{\text{star}}$.

We get $\sigma_{\text{ERV}} = 0,0164(0,0167)$ SF-A (SF-B)
 $\sigma_{\text{LRV}} = 0,0489$ for the SDSS E-sample.

⇒ **The scatter of the observed FP probably requires a contribution from stellar population effects**

EVOLUTION AT $z < 1,5$

SOME OBSERVATIONAL RESULTS

A set of observations suggest that Es formed according with the *monolithic collapse scenario*

- ♠ A population of massive, relaxed spheroids with old stellar populations (i.e., formed at a redshift of $z_f > 2,4$) was already at place by $z \sim 1,5 - 2$ or even earlier (Cimatti et al. 2002, 2004; Stanford et al. 2004; Mobasher et al. 2005).
- ♠ This population lacks of significant structural and dynamical evolution (Treu & Koopmans 2004; Trujillo et al. 2004; McIntosh et al. 2005).
- ♠ Their average luminosity evolution is consistent with a passive evolution of their stellar populations, that could explain the evolution of the FP relation (keeps the tilt) (van Dokkum et al. 2001; ...; di Serego-Alighieri et al. 2005)
- ♠ In E galaxies, most SF occurred: i), at high z s, ii), on short timescales, and, moreover, iii) at higher z s and on shorter timescales for increasing E mass (Cadwell et al. 2003; Bernardi et al. 2003; Thomas et al. 2005; R. Jiménez's talk)

HOWEVER, another set of recent observations suggest that *mergers* at z s below $\sim 1,5 - 2$ could have played an important role in E assembly

- ♠ The signatures of merging observed by the moment out to intermediate z s (Le Fèvre et al. 2000; Conselice 2003; Cassata et al. 2005; Bell et al. 2005)
- ♠ The growth of the total stellar mass bound up in bright red galaxies by a factor of ~ 2 since $z = 1$ (Bell et al. 2004; Conselice et al. 2005; Faber et al. 2005)
- ♠ The need for a young stellar component in some E galaxies, in particular the existence blue cores in relaxed systems (van Dokkum & Ellis 2003; van der Wel et al. 2004; Menanteau et al.)

Paradoxical and challenging!!!

Demands:

- Passive-evolving stellar populations and a FP that preserves its tilt.
- Mass assembly is an on-going process and some SF is still on at $z < 1,5$.

WHAT ABOUT ELOs?

Structural and dynamical evolution: ELO SAMPLES

SF-A type, three snapshots (E-Z0, E-Z1, E-Z1.5)

Measuring Structural and Dynamical Evolution

- Look for evolution in the intrinsic 3D variable space

$$E \equiv \log M_{\text{bo}}^{\text{star}}$$

$$r \equiv \log r_{\text{e,bo}}^{\text{star}}$$

$$v \equiv \log \sigma_{3,\text{bo}}^{\text{star}}$$

through the 3×3 correlation matrix in these variables.

- We found that

$$E - \tilde{E}_z = \alpha^{3\text{D}}(z)(r - \tilde{r}_z) + \beta^{3\text{D}}(z)(v - \tilde{v}_z), \quad (2)$$

shows the plane viewed edge-on.

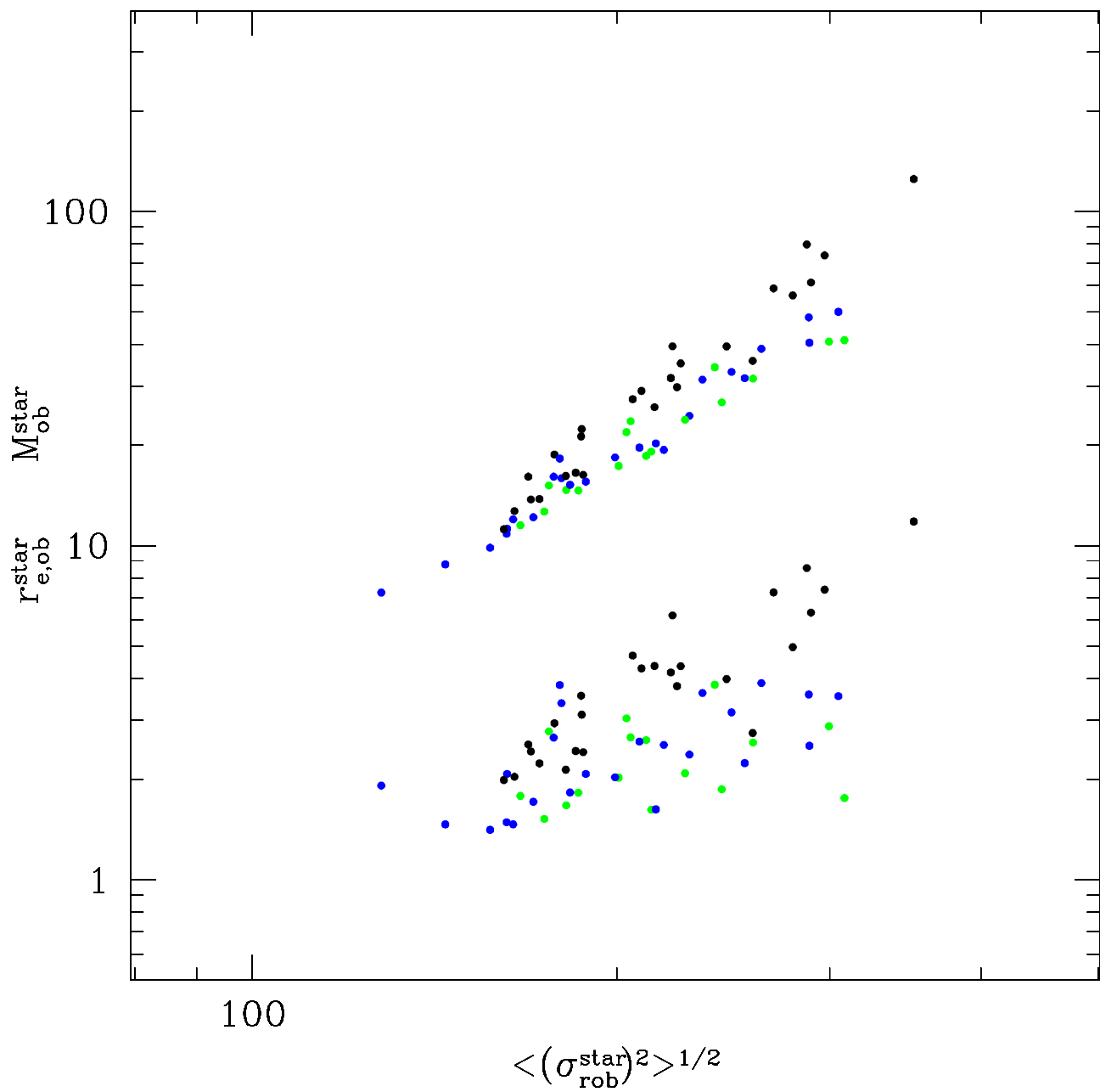
- $(\tilde{E}_z, \tilde{r}_z, \tilde{v}_z)$, the center of mass at z , grows as z decreases.

- But it moves on the $z = 0$ plane, within the scatter
- And $\sim 95\%$ of ELOs in E-Z1 and E-Z1.5 samples keep on the plane of the E-Z0 sample (within $1\sigma_{\text{Erv}}$)

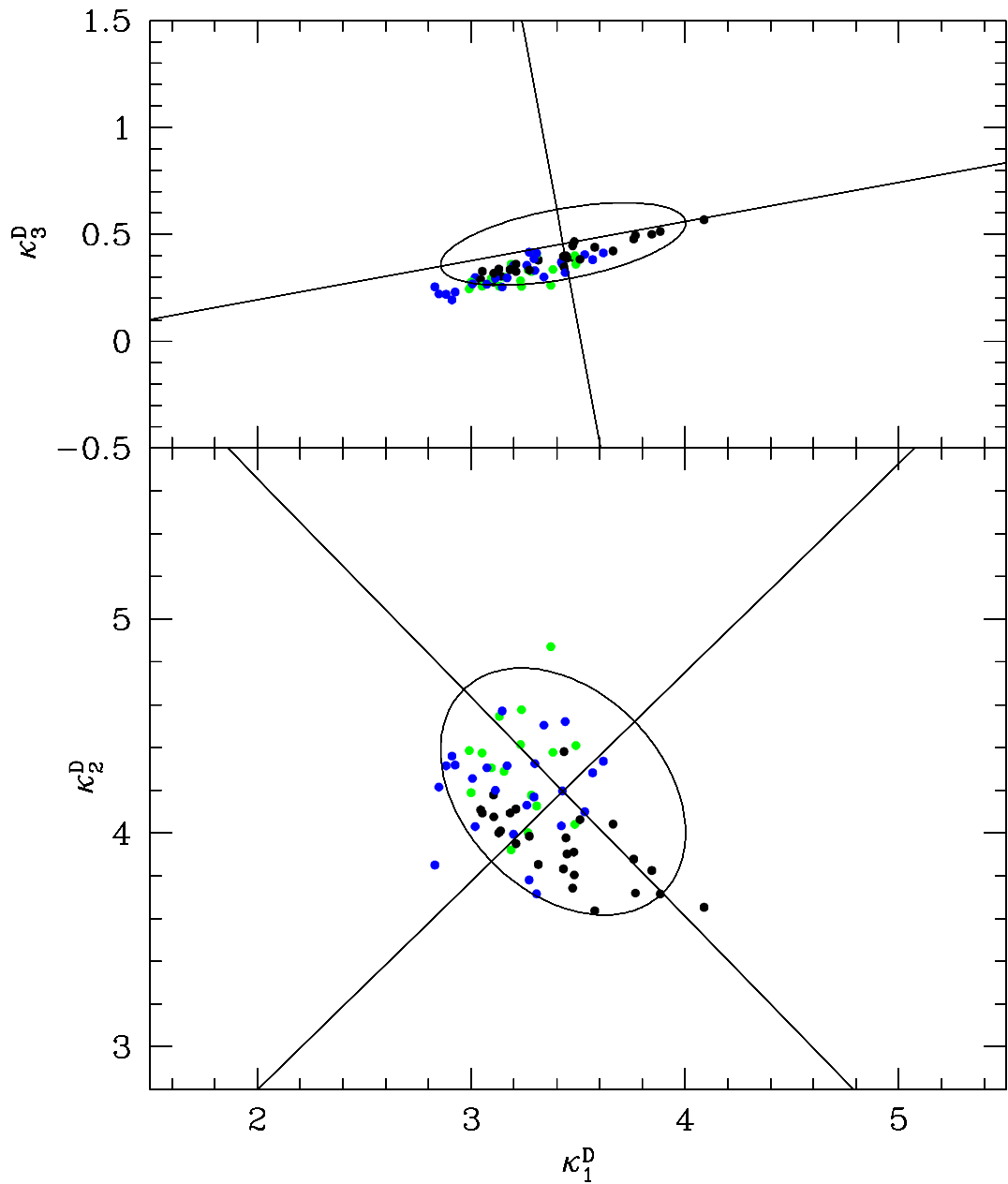
ELOs grow but they keep their DYNAMICAL FP !!

Cuadro 1: THE DYNAMICAL FPs AT DIFFERENT Z_s

Sample	#	\tilde{E}_z	\tilde{r}_z	\tilde{v}_z	α_z^{3D}	β_z^{3D}	$\sigma_{\text{Erv},z}$
EA-Z0	26	10.993	0.746	2.335	0.427	2.066	0.011
EA-Z1	24	10.812	0.519	2.303	0.251	2.098	0.011
EA-Z1.5	16	10.860	0.495	2.333	0.307	2.013	0.013



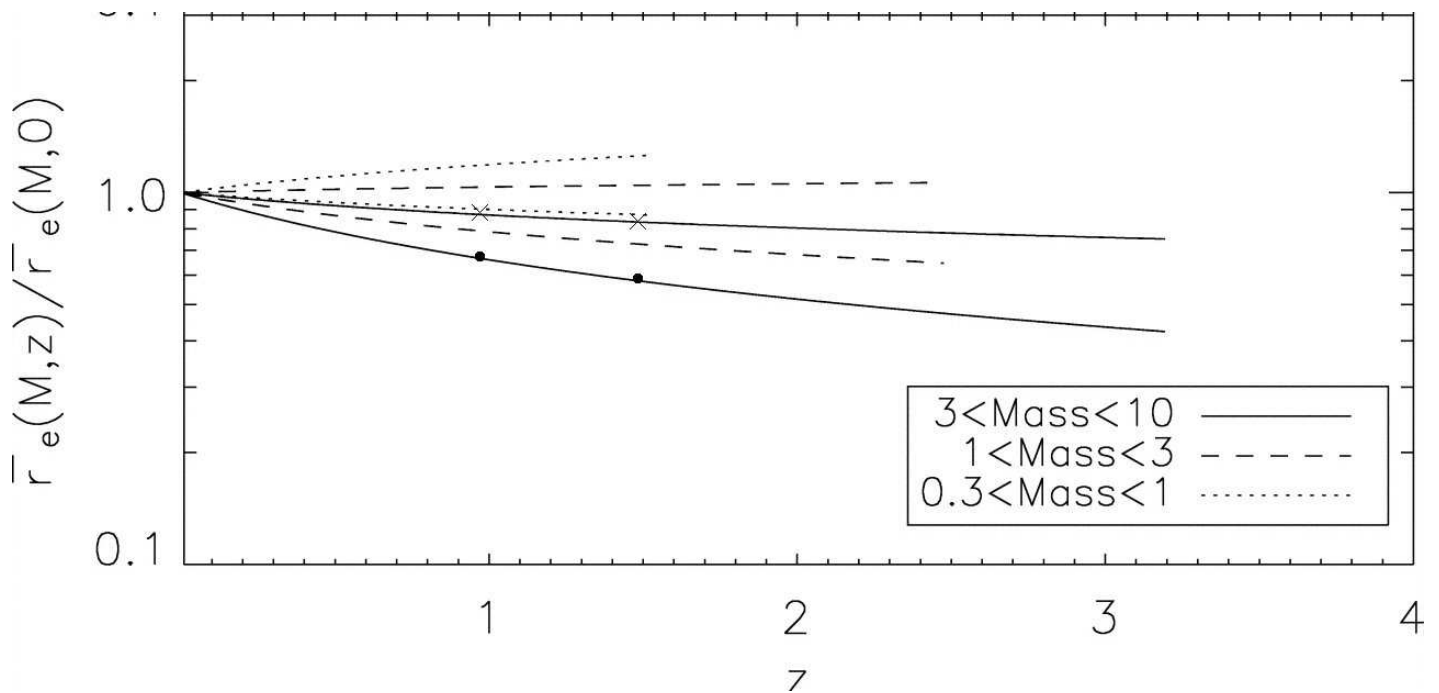
Two projections of the intrinsic 3D variable space for the E-Z0 (black), E-Z1 (green), E-Z1.5 (blue) samples.



The dynamical FP viewed edge-on (top) and face-on (bottom) for E-Z0 (black), E-Z1 (green), E-Z1.5 (blue). We also draw the respective concentration ellipses (with their major and minor axes) for the SDSS early-type galaxy sample from Bernardi et al. (2003b) in the z -band at $z = 0$

COMPARING WITH OBSERVATIONS

Size evolution at fixed stellar mass (Trujillo et al. 2004)



The quotients $Q(z)$ of the average values of the projected stellar half-mass radii of ELOs in E-Z1 and E-Z1.5 samples over that of ELOs in E-Z0 sample, in two stellar mass bins

Cuadro 2:

Stellar mass bin	$Q(z = 1)$	$Q(z = 1,5)$
B1	0.68	0.57
B2	0.91	0.84

STELLAR AGE EFFECTS

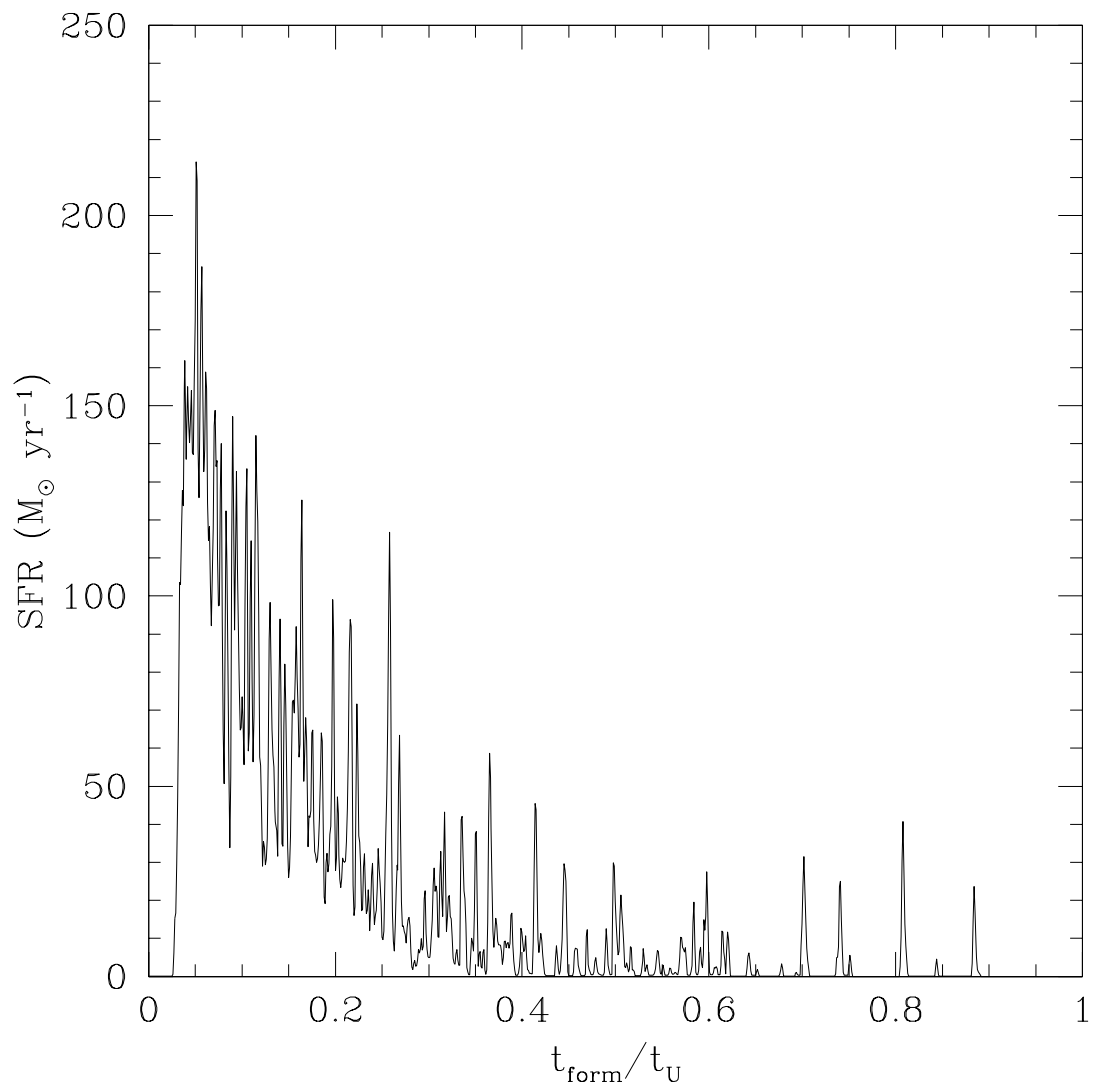
Age distribution of stellar populations in Es

- ♠ Key piece in the puzzle of galaxy formation and evolution
- ♠ Recently, break age-metallicity degeneracy possible (spectral indices $H_\beta, H_\gamma, H_\delta$)
- ♠ Improved E age determinations through evolutionary synthesis models (Maraston 2003)

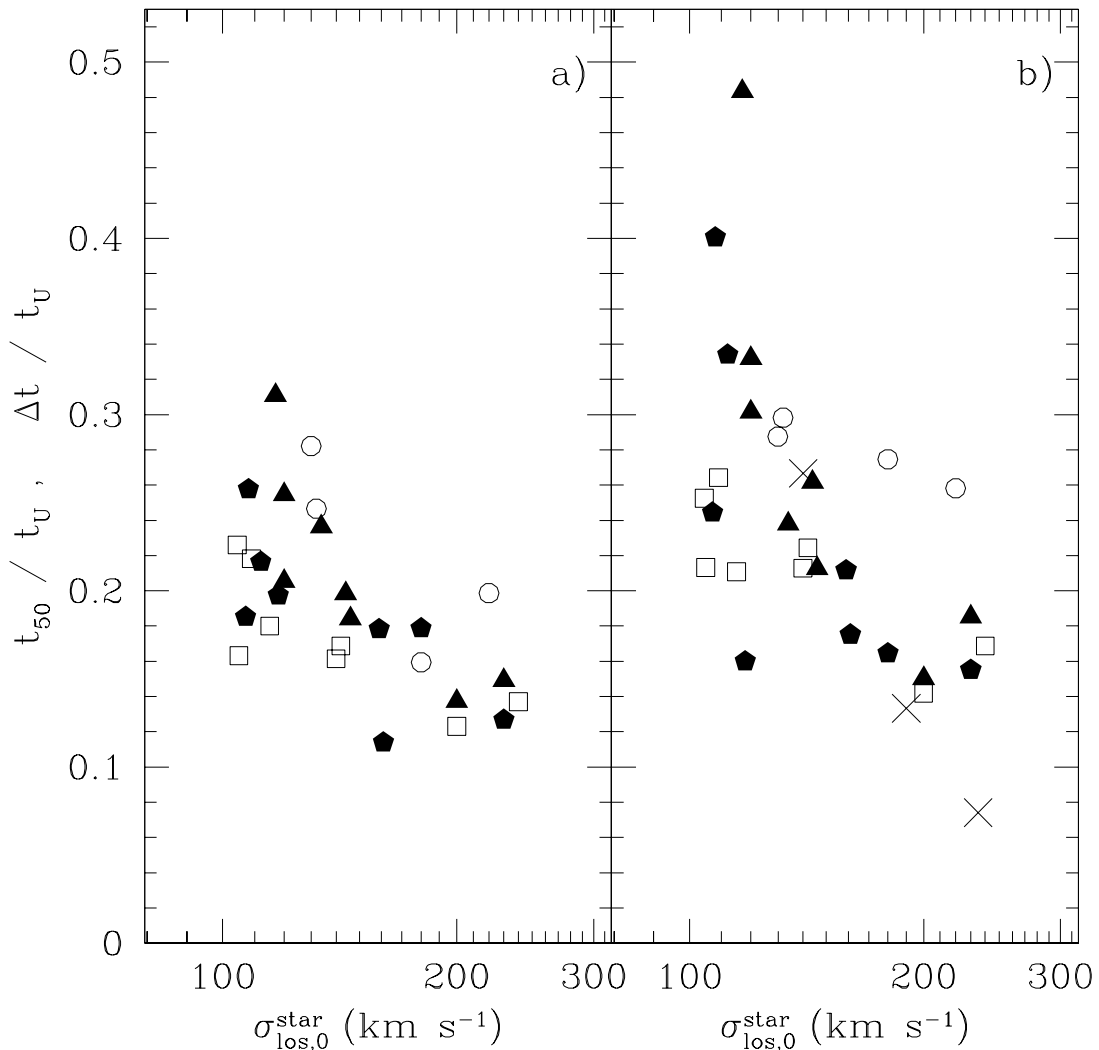
FIND: DOWNSIZING

Age distribution of stellar populations in Es has older averages and narrower spreads with increasing $\sigma_{\text{los},0}^{\text{star}}$ (Thomas, Maraston & Bender 2002; Jiménez et al. 2004; Thomas et al. 2005)

Is this consistent with the clustering paradigm?



Star formation rate history of a massive ELO as a function of universe age in units of the current universe age = Stellar age distribution.



(from Domínguez-Tenreiro et al. 2004, ApJL) (a) Age of the universe in units of the current universe age at which the 50 per cent of the total ELO stellar mass at $z = 0$ was already formed, versus their corresponding stellar central l.o.s. velocity dispersion. Filled triangles and pentagons stand for S16 and S17 ELOs; open squares and circles for S14 and S26 ELOs, respectively. (b) Same as (a) for the width $\Delta t \equiv t_{75} - t_{10}$ of the stellar population age distribution. Crosses are width estimations from elliptical data (Thomas et al. 2002)

DOWNSIZING:

More massive (M_{vir}) ELOs form more stars and earlier on than less massive ones.

Close connection between SF and gravo-hydrodynamical processes

- Important dynamical activity.
- SUGGESTS: Distinguish between SF history and mass assembly history: later merger events do not necessarily result into important SBs

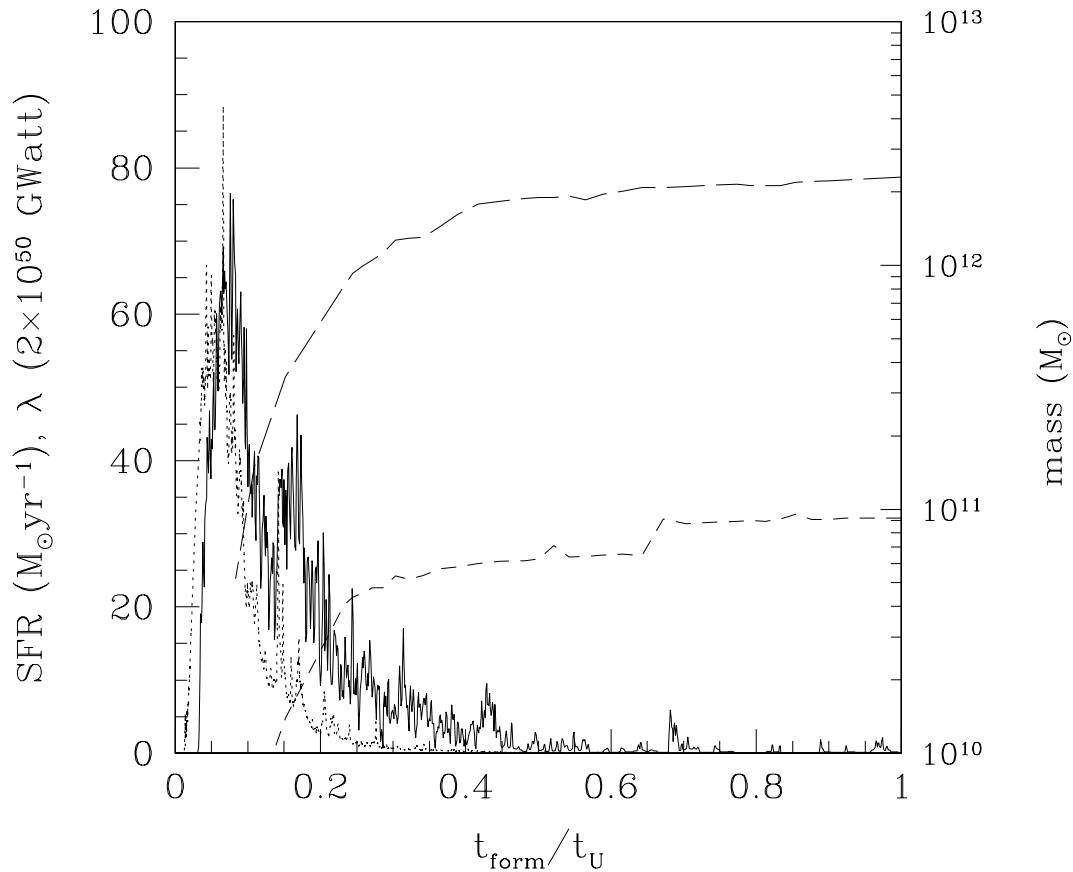
DRY MERGING (as suggested by Bell et al. 2005 from observations)

ELO MASS ASSEMBLY FROM HS

Analytical models, as well as N-body simulations indicate that two different phases operate along halo mass assembly (Wechsler et al. 2002; Zhao et al. 2003; Salvador-Solé et al. 2005):

- ♠ first, a violent fast one, where the mass aggregation rates are high,
- ♠ then, a slower one, with lower mass aggregation rates

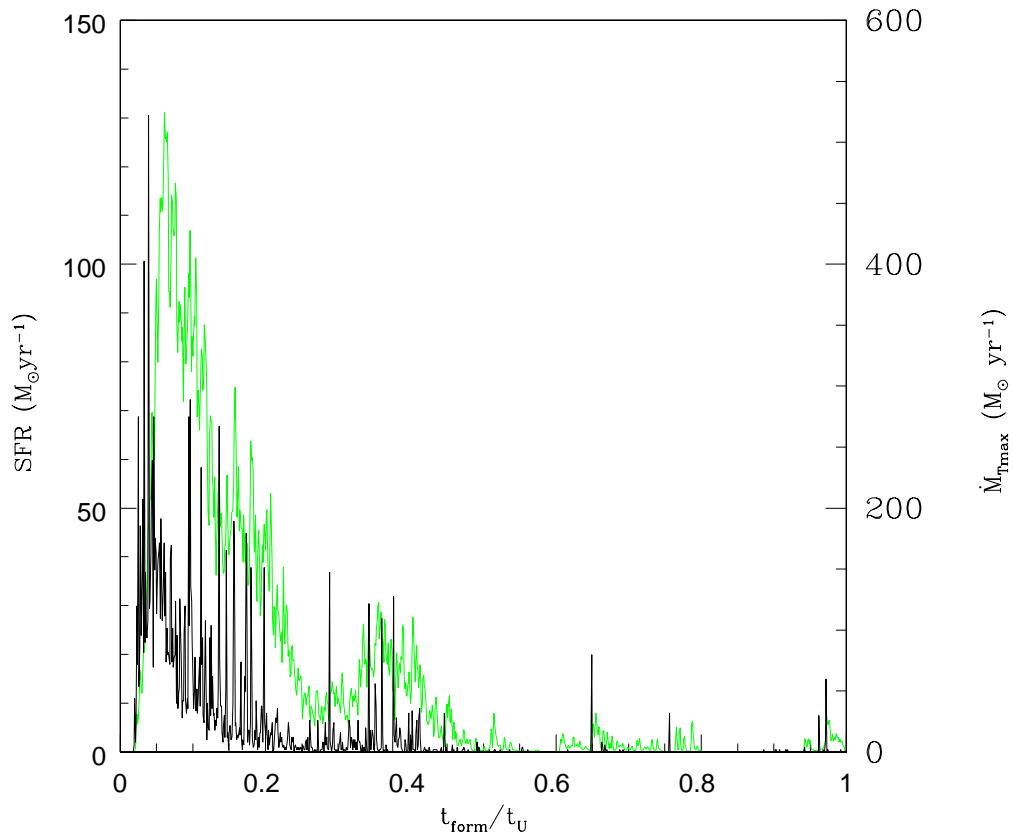
WHAT ABOUT BARYONS?: HYDRO SIMULATIONS



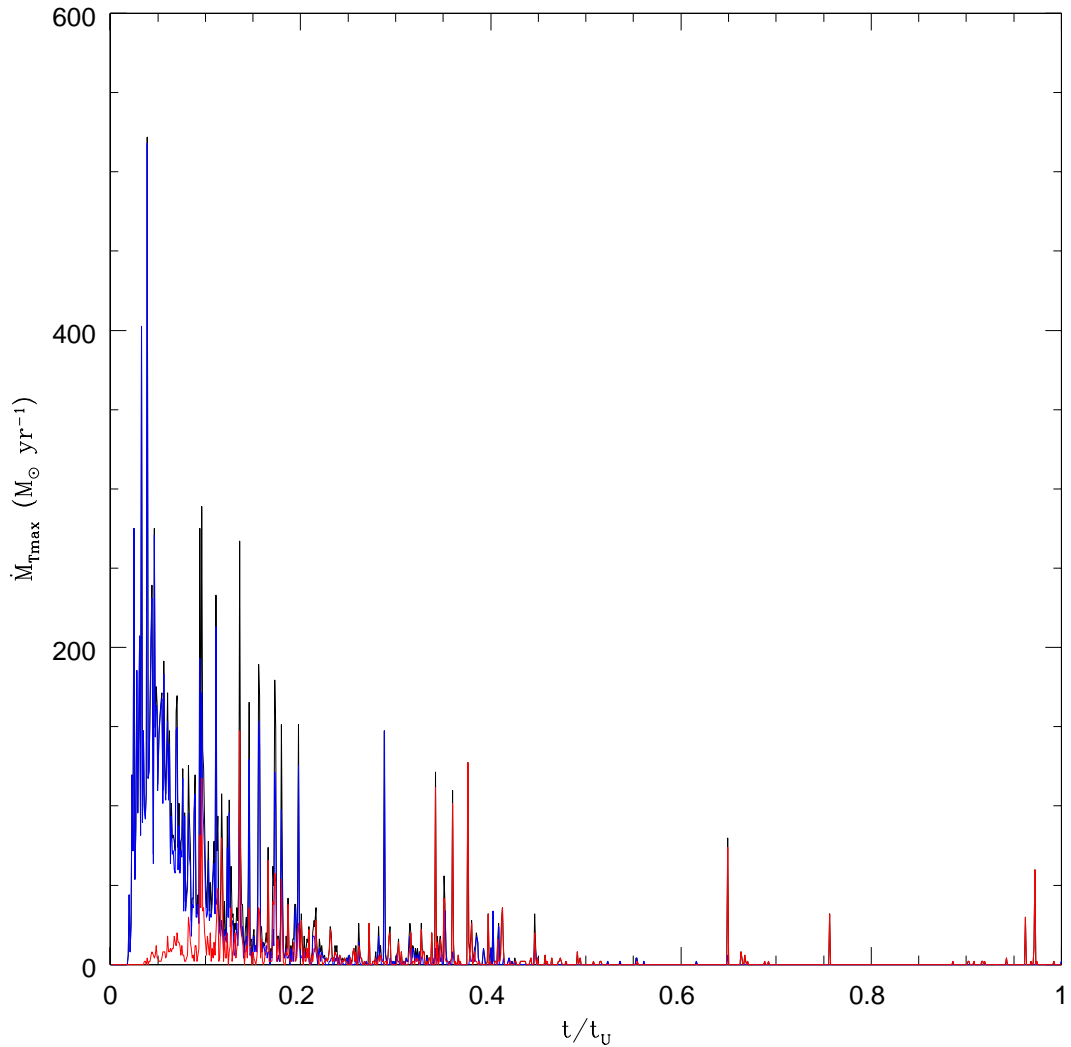
The cooling rate history λ (point line) and the star formation rate history (full line) of a typical ELO in the simulations. We also plot its Mass Aggregation Tracks, both for cold baryons (i.e., stars and cold gas) and total mass. The fast (left) and slow (right) phases of mass aggregation are clearly shown. The cooling rate history is a courtesy by F. Martínez-Serrano.

HOW DO ELLIPTICALS GET THEIR GAS

- ♠ Identify cold baryon particles at $z = 0$ in a given ELO.
- ♠ For each of them, measure its "historical" MAXIMUM TEMPERATURE, T_{\max}
- ♠ Reckon the universe age, t_{\max}/t_u , when this happened.
- ♠ Determine the amount of gas mass, $\Delta M_{\text{gas}}^{\max}(t)$, that reaches its T_{\max} in the time interval $t, t + \Delta t$
- ♠ Plot $\Delta M_{\text{gas}}^{\max}(t)/\Delta t$.



$\Delta M_{\text{gas}}^{\text{max}}(t)/\Delta t$ versus t/t_U , (black) compared with the SFRH (green) for a typical massive ELO



$\Delta M_{\text{gas}}^{\text{max}}(t)/\Delta t$ versus t/t_{u} for particles with $T_{\text{max}} < 3 \times 10^5$ (cold accretion mode, blue) and $T_{\text{max}} > 3 \times 10^5$ (hot accretion mode, red), compared with the total (black); consistent with Keres et al. 2005.

STRONG CORRELATION among:

$$\Delta M_{\text{gas}}^{\text{max}}(t) / \Delta t$$

Dissipation rate history

SFRH

SHOCK FORMATION

- ♠ Most dissipation takes place at the early violent phase, causing the $M_{\text{bo}}^{\text{star}}$, $r_{\text{e,bo}}^{\text{star}}$, and $\sigma_{3,\text{bo}}^{\text{star}}$ parameters to settle down to the DP, and, moreover, the transformation of most of the available gas into stars.
- ♠ In the subsequent slow phase, ELO stellar mass growth preferentially occurs through non-dissipative processes, so that the DP is preserved and the ELO star formation rate considerably decreases.

Understanding the Fundamental Plane Lack of Evolution

HOWEVER...

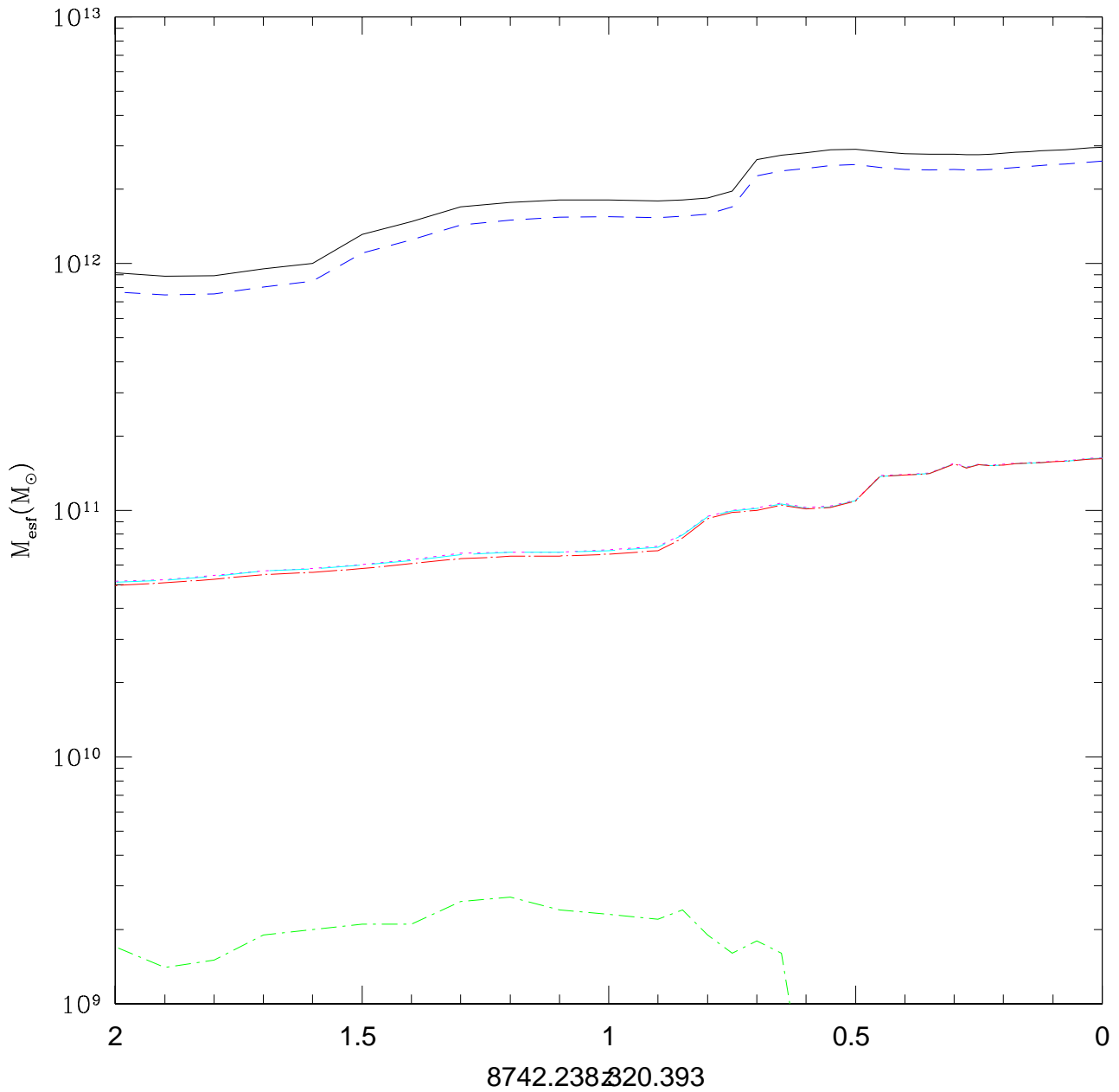
On-going ELO mass assembly at $z < 2$ through

- Major mergers \Rightarrow Almost dissipationless, carry DM & stars
- Minor mergers \Rightarrow Carry DM, stars & gas
- Gas accretion (low rate)

On-going STELLAR mass growing through

- Newly incorporated pre-existing stars from major mergers
- Newly incorporated pre-existing stars from minor mergers

- New born stars from gas



The MAT for an ELO in the slow phase of mass aggregation, for total, dark, cold baryons, stellar and gaseous mass. A major and a minor merger can be appreciated, as well as gas accretion and its consumption in a small SB

CAN EXPLAIN DYNAMICAL ACTIVITY at intermediate z s

Blue cores, Menanteau et al. 2004

Kinematical peculiarities shown by E population

Stellar mass fraction contributed by spheroids increases as z decreases, Conselice et al. 2004

SUMMARY

A very simple scenario for galaxy assembly...

- INITIAL CONDITIONS Montecarlo realization of the field of primordial fluctuations to a Λ CDM cosmological model
- EVOLUTION under gravity, hydro equations (conservation laws)
- Cooling effects
- Simple model for SF: parameterization + Kennicutt-Schmidt-law-like algorithm, containing our ignorance about SF process at subresolution scales

We got

- Structure & Dynamics OK; except for a possible excess of dissipation in the smaller ELOs. FP at $z = 0$ OK.
- Structural and dynamical evolution consistent with observations.
- Correlation mean stellar age- velocity dispersion ; Age dispersion of stellar populations in ETGs OK.

We find

- Most dissipation involved in ELO formation takes place at the early violent phase of their halo evolution \Rightarrow Strong SFB and DP
- In the slow phase most ELO mass growth preferentially occurs through non-dissipative processes \Rightarrow The SFR considerably decreases and the DP is preserved.
- Some SF can be still on in the low phase.
- Most stars formed at high z while they are assembled later on (similar conclusions from semi-analytical model grafted to the Millennium Simulation, de Lucia et al. 2005).

\Rightarrow

SCENARIO FOR E FORMATION FROM SIMULATIONS

- Unified scenario where most current observations on E can be interrelated.
- Advantage: dark mass and gas aggregation histories result from simple physical laws acting on generic initial conditions.